J. Biochem. 123, 358-368 (1998)

Genomic Structures and Chromosomal Location of p91, a Novel Murine Regulatory Receptor Family[1]

Yumi Yamashita,*,† Daisuke Fukuta,* Atsushi Tsuji,‡ Akira Nagabukuro,‡ Yoichi Matsuda,‡ Yasuhiro Nishikawa,* Yukiya Ohyama,* Hitoshi Ohmori,* Masao Ono,*,†,2 and Toshiyuki Takai*,†,2,3

*Department of Biotechnology, Faculty of Engineering, Okayama University, Tsushima-Naka, Okayama 700; †Core Research for Evolutional Science and Technology (CREST), Japan Science and Technology Corporation (JST); and ‡Laboratory of Animal Genetics, School of Agricultural Sciences, Nagoya University, Chikusa-ku, Nagoya 464-01

Received for publication, October 22, 1997

Recently, we found a novel murine cell-surface glycoprotein, designated as p91, expressed mainly in myeloid cells such as macrophages and mast cells. The molecule has six immunoglobulin-like extracellular domains, a transmembrane segment, and a cytoplasmic tail containing four immunoreceptor tyrosine-based inhibition motif (ITIM) or ITIM-like sequences, resembling the structural features of human killer-cell inhibitory receptors (KIR). Here we show that p91 comprises a polymorphic gene family, harboring one potent inhibitory-type p91 and at least two other p91 genes. Tyrosine-phosphorylated, but not nonphosphorylated, synthetic peptides matching the third ITIM and the fourth ITIM-like sequences, respectively, found in the cytoplasmic portion of p91A, the sole inhibitory-type p91, were associated with the tyrosine phosphatases, SHP-1 and SHP-2. In addition, the phosphotyrosyl peptide matching the third ITIM sequence also bound the inositol 5-phosphatase, SHIP. These results support the notion that p91A may function as an inhibitory cell-surface molecule against cell activation. The p91 genes were shown to be clustered in the proximal region of mouse chromosome 7, a syntenic position of human chromosome 19 where the genes for the KIR family are found. A human cDNA clone cross-hybridizing to a murine p91 probe was isolated from a human spleen cDNA library, and was found to code for a molecule quite similar to members of the immunoglobulin-like transcript (or ILT) family. The gene was found to be located on human chromosome 19q13.3-13.4. These results establish the existence of a novel set of potent regulatory receptors in mouse and man, similar but different from the KIR family.

Key words: immunoregulation, ITIM, KIR, SHP, SHIP.

The regulation of cellular responses in the immune system by a group of receptors for the immunoglobulin Fc portion (FcR) is one of the suitable examples that depict how cells are controlled by their cell surface activating and inhibitory receptors (for reviews, see Refs. *1* and *2*). Type III FcR for IgG (FcγRIII) is an example of an activating FcR, composed of a ligand binding α subunit and a CD3ζ or FcRγ chain homodimer or a ζ-γ heterodimer containing one or two sets of an immunoreceptor tyrosine-based activation motifs (*3*), which recruits a *src*-homology 2 (SH2)-containing protein tyrosine kinase, Zap-70, or Syk, after phosphorylation of the tyrosine residues, and transmits the activation signal to the cell interior (*4-6*). On the other hand, an inhibitory FcR, FcγRIIB, possesses an immunoreceptor tyrosine-based inhibitory motif (ITIM) (*7-10*) in its cytoplasmic domain, whose consensus sequence is V/I-X-Y-X-X-L/V (*11*). The stimulation of B cells with an intact anti-membrane Ig antibody induces co-crosslinking between the B-cell antigen receptor and FcγRIIB on the cell surface, resulting in attenuated B cell signal transduction due to the binding of SH2-containing proteins to the phosphorylated ITIM of FcγRIIB in the cell interior (*9, 10*). The proteins that become associated with the phosphorylated ITIM

[1] This work was supported by research grants from the Ministry of Education, Science, Sports and Culture of Japan (to T. T., and Y. M.), and CREST, Japan Science and Technology Corporation (to T. T.). The nucleotide sequences reported in this paper will appear in the DDBJ/EMBL/GenBank DNA databases under accession numbers: p91A, AF040946, AF040947, AF040948, AF040949, AF040950, AF040951, AF040952, and AF040953; p91B, AF041035; p91C, AF041036; a human p91, AF041034.

[2] Present address: Department of Molecular Embryology, Institute of Development, Aging and Cancer, Tohoku University, Seiryo 4-1, Aoba-ku, Sendai 980-8575.

[3] To whom correspondence should be addressed at the present address. Tel: +81-22-717-8501, Fax: +81-22-717-8505, E-mail: tostakai@idac.tohoku.ac.jp

Abbreviations: bp, base pair(s); BrdU, bromodeoxyuridine; DAPI, 4, 6-diamidino-2-phenylindole; FcR, Fc receptor; FcγR, IgG Fc receptor; FCS, fetal calf serum; FISH, fluorescence *in situ* hybridization; Ig, immunoglobulin; ILT, immunoglobulin-like transcripts; ITIM, immunoreceptor tyrosine-based inhibitory motif; kb, kilobase(s); KIR, killer-cell inhibitory receptor; MAFA, mast cell function-associated antigen; NK, natural killer; PIR, paired inhibitory receptor; RFLV, restriction fragment length variant; RT-PCR, reverse transcription-polymerase chain reaction; SDS-PAGE, sodium dodecyl sulfate-polyacrylamide gel electrophoresis; SH2, *src*-homology 2; SHIP, SH2-containing inositol polyphosphate 5-phosphatase; SHP, SH2-containing tyrosine phosphatase.

sequence of FcγRIIB were shown to be an SH2-containing tyrosine phosphatase (SHP)-1 (*12*) and an SH2-containing inositol polyphosphate 5-phosphatase (SHIP) in B cells (*13*), whereas in mast cells SHIP was shown to be preferentially recruited to FcγRIIB (*13*).

This mode of inhibition is also the case for killer-cell inhibitory receptors (KIR) expressed by natural killer (NK) cells and a T cell subset (for reviews, see Refs. *14-17*). Human KIR such as p58 and p70 are type I transmembrane glycoproteins belonging to the Ig superfamily (*18-20*). In contrast, another type of KIR including human CD94 (*21*) and mouse Ly-49 (*22*) are type II transmembrane glycoproteins with the C-type lectin structure. Despite these quite different structures, both types of KIR recognize allelic groups of the MHC class I molecules on the target cells. The engagement of these inhibitory receptors results in a dominant negative signal that prevents lysis of the target cells. Tyrosine phosphorylation of their ITIM has been shown to be necessary for the interaction with SHP-1 at p58 (*11, 23*) as well as at Ly-49 (*24*).

Recently, we found that mouse macrophages and mast cells express a novel type of molecule, designated as p91 (*25*), whose structural characteristics are quite similar to those of human p58 and p70 KIR, and mouse gp49B1 (*26, 27*), and which was recently identified as a murine KIR-like inhibitory molecule expressed on mast cells (*28*) and NK cells (*29, 30*). The cytoplasmic portion of p91 has four ITIM-like sequences and shows exceedingly high sequence homology to gp49B1. p91 has been verified to be expressed as 110- and 130-kDa protein species on the surface of COS-1 cells transfected with p91 cDNA (*25*). Although the physiological role of the p91 molecule is unknown, it is possible that p91 functions as an inhibitory receptor on myeloid cells such as macrophages. Thus, elucidation of the physiological ligand for p91 as well as the biochemical characteristics of the inhibitory cascade of the molecule should be valuable for understanding the control mechanisms of cells in the immune system. We show here that p91 comprises a multigene family, which includes a unique inhibitory p91A gene and at least two other p91 genes, p91B and p91C, and that the phosphotyrosyl ITIM or ITIM-like sequences of the p91A protein actually bind SH2-containing phosphatases. We also show that human p91-like molecules may be isoforms of the Ig-like transcript (ILT) found very recently (*31, 32*).

MATERIALS AND METHODS

Screening and Isolation of Genomic and cDNA Clones—For the isolation of mouse genomic DNA clones, a 1.0-kilobase-pair (kb) *Eco*RI-*Xho*I fragment from cDNA-55, a mouse p91A cDNA clone (*25*), was labeled with a random primer labeling kit (Takara Shuzo, Otsu) and [α-^{32}P]dCTP (specific activity, ~3,000 Ci/mmol, Amersham), and was used to screen 8×10^5 plaques from a genomic library constructed from 129/Sv mouse liver DNA in the λFixII vector (Stratagene) under stringent conditions (*33*). Five positive signals were detected, and plaque purification was completed for the five clones. The isolation of cDNA clones for p91 through the screening of a B10.A mouse cDNA library prepared from thioglycollate-elicited macrophages was described previously (*34*). For the isolation of cDNAs for human p91-like molecules, a 1,491-base-pair (bp) *Eco*RI fragment from cDNA-55 (*25*) was used to screen 5×10^5 plaques from a human cDNA library constructed from a 20-year-old Caucasian female spleen in the λgt10 vector (Clontech, Palo Alto, CA) under less-stringent conditions (hybridization in 35% formamide at 42°C and washing in 0.3×SSC at 42°C). Nineteen positive signals were detected, four of which were also positive as to hybridization with a 581-bp *Sac*I-*Hin*fI probe coding for the pretransmembrane and transmembrane domains, and the N-terminal portion of the cytoplasmic domain of p91A. Plaque purification was completed for these 4 doubly-positive clones.

DNA Sequencing and Computer Analysis—The genomic DNA and cDNA clones were subcloned into plasmid pUC19 or pBluescript (Stratagene), and then sequenced by the dideoxy chain termination method (*35*) using a Cy5 AutoRead sequencing kit and an ALFexpress DNA sequencer (both from Pharmacia Biotech). A homology search of the GenBank™ and SwissProt data-bases, and alignment of the nucleotide and amino acid sequences were performed with the aid of GenomeNet Japan and the Genetyx program (Software Development, Tokyo).

Reverse Transcription-Polymerase Chain Reaction (RT-PCR) Analysis—For the detection of mRNA for p91, total RNA isolated from various mouse tissues (*36*) was subjected to RT-PCR analysis using the following primers: the forward primer, 5′-GTGCAGCCTAACCACACAGTGC-3′ (corresponding to nucleotide residues 1582-1603 of p91A) (*25*), and the backward primer, 5′-TCTGCTAGGCATCC-TGGCAGGC-3′ (residues 2533-2554 of p91A) or 5′-TGG-GTCTGTCTATGGCTTCGCC-3′ (residues 1931-1952 of p91B/C) for the detection of p91A or p91B/C, respectively. First strand cDNA synthesis was performed using 0.5 μg of total RNA using a first strand cDNA synthesis kit (Boehringer Mannheim) with an oligo(dT) primer. One-fourth of the reverse-transcribed RNA mixture was incubated with each of the primer pairs described above and then subjected to 35 cycles of amplification using the standard PCR protocol. The amplified product was separated on a 2% NuSieve 3:1 agarose gel (FMC BioProducts, Rockland, ME) and visualized by ethidium bromide staining.

Cell Culture—Thioglycollate-elicited peritoneal macrophages and bone marrow-derived mast cells were prepared as described previously (*34*). NK cells were induced from splenocytes from 6- to 8-week-old C57BL/6 mice with IL-2 as described (*34*). Peritoneal residential cells were harvested by peritoneal lavage. Various cells from mouse tissues, including splenocytes, thymocytes, and mesenteric lymph node cells, were prepared by crushing the tissues with the hub of a syringe and a stainless tea filter in phosphate-buffered saline (PBS) without Ca^{2+} or Mg^{2+}. T cell-depleted splenocytes were prepared by treating spleen cells with anti-Thy1.2 plus complement. B lymphoma cell line A20 (*37*) was maintained in RPMI-1640 plus 10% heat-inactivated fetal calf serum (FCS) and 50 μM β-mercaptoethanol.

Affinity Isolation of Cellular Proteins and Immunoblot Analysis—For the detection of cellular proteins that bind to the four ITIM-like sequences found in the cytoplasmic portion of p91A, eight biotinylated peptides were synthesized: the sequences being TQEESLYASVED-amide (in the one-letter code, designated as Y1, corresponding to amino acid residues 684-695), TQEESL[pY]ASVED-

amide (pY1), DPQGETYAQVKP-amide (Y2, residues 713-724), DPQGET[pY]AQVKP-amide (pY2), ESQDVTYAQLCS-amide (Y3, residues 765-776), ESQDVT[pY]AQLCS-amide (pY3), PEEPSVYATLAA-amide (Y4, residues 796-806), and PEEPSV[pY]ATLAA-amide (pY4), where each N-terminal residue is biotinylated, and [pY] denotes a phosphotyrosine residue.

Macrophages were solubilized by adding extraction buffer (50 mM Tris-HCl, pH 7.4, 1% Nonidet P-40, 150 mM NaCl, 1 mM phenylmethyl sulfonyl fluoride, 10 μg/ml aprotinin, 20 μg/ml leupeptin, 1 mM disodium EDTA, 10% glycerol, and 5 mM orthovanadate) to the cell pellet. Where indicated, the cells were stimulated for 15 min at 37°C in DMEM plus 10% FCS with 0.03% H_2O_2 and 100 μM sodium orthovanadate, which pharmacologically induces protein tyrosine phosphorylation (*38*). The extract was then incubated on ice for 10 min, and the insoluble material was removed by centrifugation at 15,000×g for 15 min at 4°C. The soluble extract was precleared with 1.0 ml of avidin-Sepharose FF beads/10^7 cell eq (Pharmacia Biotech) in extraction buffer. The beads were removed by centrifugation at 15,000×g for 5 min, and the extract was then incubated for 18 h at 4°C with 0.5 ml of the biotinylated peptides/10^7 cell eq, followed by precipitation with avidin-Sepharose beads. The pelleted beads were washed four times by centrifugation in extraction buffer containing 0.1% gelatin but devoid of aprotinin and leupeptin, resuspended in sodium dodecyl sulfate-polyacrylamide gel electrophoresis (SDS-PAGE) sample buffer (63 mM Tris-HCl, pH 6.8, 2% SDS, 5% 2-mercaptoethanol, 10% glycerol, 0.002% bromphenol blue, and 4 M urea), boiled for 1 min to liberate immunoprecipitated materials, and then centrifuged. The immunoprecipitates or cell lysates were subjected to SDS-PAGE separation on a 7.5% gel, and then transferred to a polyvinylidine difluoride membrane (Immobilon P; Millipore) using a Milliblot electroblotting system. The blot was first blocked with 5% nonfat dry milk (Carnation) in PBS and 0.3% Tween 20, incubated with 0.5 μg/ml anti-SHP-1 rabbit IgG or anti-SHP-2 rabbit IgG (both from Santa Cruz Biotechnology, Santa Cruz, CA), or a 1:2,000 dilution of anti-SHIP antiserum (kindly provided by Dr. K.M. Coggeshall, Ohio State Univ.), and then washed three times in PBS/Tween. The blot was then treated with a peroxidase-conjugated mouse anti-rabbit IgG (clone RG-16; Sigma) and detected as enhanced chemiluminescence (Amersham).

Chromosome Preparation and Fluorescence In Situ Hybridization (FISH)—The direct R-banding FISH method was used for chromosomal assignment of the mouse and rat p91 genes. Preparation of R-banded chromosomes and FISH were performed as described (*39, 40*). A mitogen-stimulated splenocyte culture was synchronized by means of a thymidine block, and the incorporation of 5-bromodeoxyuridine (BrdU) during the late replication stage was monitored for differential replication staining after the release of excess thymidine. R-band staining was performed by exposure of chromosome slides to UV light after staining with Hoechst 33258. The chromosome slides were hardened at 65°C for 2 h, and then denatured at 70°C in 70% formamide in 2×SSC and dehydrated in a 70-85-100% ethanol series at 4°C.

A mouse 0.9-kb p91A cDNA fragment inserted into the *Eco*RI site of pUC19 and the mouse 16-kb genomic DNA fragment from the p91C gene inserted into the *Xho*I site of λFixII were labeled by nick translation with biotin 16-dUTP (Boehringer Mannheim) following the manufacturer's protocol. The labeled DNA fragment was ethanol-precipitated with salmon sperm DNA and *Escherichia coli* tRNA, and then denatured at 75°C for 10 min in 100% formamide. A ten times amount of Cot-1 DNA was added when the genomic DNA fragment was used as a probe. The denatured probe was mixed with an equal volume of a hybridization solution to give final concentrations of 50% formamide, 2×SSC, 10% dextran sulfate, and 2 mg/ml BSA (Sigma). A 20 μl mixture containing 250 ng labeled DNA was put on a denatured slide, which was covered with parafilm and then incubated overnight at 37°C. The slides were washed for 20 min in 50% formamide in 2×SSC at 37°C, and then in 2×SSC and 1×SSC for 15 min each at room temperature. After rinsing in 4×SSC, the slides hybridized with the genomic DNA fragment were incubated under a coverslip with fluoresceinated avidin (Vector Laboratories) at 1:500 dilution in 1% BSA/4×SSC for 1 h at 37°C. After washing with 4×SSC, 0.1% Nonidet P-40 in 4×SSC, and 4×SSC each for 10 min on the shaker, the slides were rinsed with 2×SSC and then stained with 0.75 μg/ml propidium iodide. The amplification method was used for the staining of the slides hybridized with the cDNA fragment. The slides were incubated, with coverslips, with an anti-biotin antibody (Vector Laboratories) at 1:500 dilution in 1% BSA/4×SSC for 1 h at 37°C. They were then washed with 4×SSC, 0.1% Nonidet P-40 in 4×SSC, and 4×SSC for 5 min each, and then stained with fluorescein-antigoat IgG (Nordic Immunology) at 1:500 dilution for 1 h at 37°C. After washing with 4×SSC, 0.1% Nonidet P-40 in 4×SSC, and 4×SSC for 10 min on the shaker, the slides were rinsed with 2×SSC and then stained with 0.75 μg/ml propidium iodide. Excitation at wavelengths of 450-490 nm (Nikon filter set B-2A) and near 365 nm (UV-2A) was used for observation. Kodak Ektachrome ASA100 films were used for microphotography.

The chromosomal mapping of a gene for a human p91-like molecule was supported by SeeDNA Biotech (Ontario, Canada). Lymphocytes isolated from human blood were cultured in α-MEM supplemented with 10% FCS and phytohemagglutinin at 37°C for 68-72 h. The lymphocyte cultures were treated with BrdU (0.18 mg/ml, Sigma) to synchronize the cell population. The synchronized cells were washed three times with serum-free medium to release the blocking and then recultured at 37°C for 6 h in α-MEM containing thymidine (2.5 μg/ml, Sigma). The cells were harvested and slides were made by means of standard procedures including hypotonic treatment, fixation, and air-drying. The 2-kb cDNA probe was biotinylated with dATP using a BRL BioNick labeling kit (15°C, 1 h) (*41*). The procedure for FISH detection was as described (*41, 42*). Briefly, slides were baked at 55°C for 1 h. After RNase treatment, the slides were denatured in 70% formamide in 2×SSC for 2 min at 70°C, followed by dehydration with ethanol. The probes were denatured at 75°C for 5 min in a hybridization mix consisting of 50% formamide and 10% dextran sulphate. The probes were loaded on denatured chromosomal slides. After overnight hybridization, the slides were washed, followed by detection and amplification. FISH signals and the 4,6-diamidino-2-phenylindole (DAPI) banding pattern were recorded sepa-

rately by taking photographs, and the assignment of the FISH mapping data with chromosomal bands was achieved by superimposing FISH signals on DAPI-banded chromosomes (*42*).

Linkage Mapping with Interspecific Backcross Mice—The recombinant animals used in this study were generated by mating males of a feral-derived mouse stock, *Mus spretus*, with C57BL/6J females, and backcrossing the F_1 females with *M. spretus* males (*43*). Whole genomic DNA prepared from kidneys of the backcross mice was digested with a restriction endonuclease. The resulting fragments were separated by electrophoresis on 0.8% agarose gels and then transferred to nylon membranes (Bio-Rad Laboratories). The mouse cDNA was used to determine the genotypes of individuals by Southern hybridization. Microsatellite DNA markers for linkage analysis were chosen according to the results of cytogenetic mapping by FISH, and purchased from Research Genetics (Huntsville, AL, USA). All PCRs were carried out in 10 μl mixtures comprising 80 ng of genomic DNA and 0.2 μmol of each oligonucleotide primer. The amplification conditions were 90°C for 3 min; and 30 cycles of 94°C for 1 min, 55°C for 1 min, and 72°C for 50 s; and then 72°C for 10 min. The PCR products were analyzed by agarose gel and polyacrylamide gel electrophoreses.

RESULTS AND DISCUSSION

Isolation of Genomic and cDNA Clones for p91—In our previous report, we described the isolation and characterization of cDNA clones for p91 from a B10.A mouse library (*25*). We assumed that p91 might be encoded by a single gene in the mouse genome because the three cDNA clones characterized in detail were found to be identical in sequence, except for deletions. On blot hybridization analysis, however, of mouse total genomic DNA samples with the p91 cDNA probe coding for an extracellular Ig-like domain, we observed four to five bands on each restriction enzyme digestion, suggesting the presence of multiple sequences identical or closely related to the p91 extracellular sequence (Fig. 1A). On the other hand, blot hybridization with a cDNA probe coding for the cytoplasmic domain suggested that the copy number of the p91 gene harboring an inhibitory sequence is only one (Fig. 1, B to D). This notion is supported by the fact that these hybridization patterns with the probe for the cytoplasmic portion were reasonably accounted for by the restriction map of the p91 gene (see below). Therefore, we next attempted to isolate several genomic clones as well as cDNA clones whose restriction maps or sequences are different from that of the initial p91, now designated as p91A, by screening a genomic library derived from 129/Sv mice, and a cDNA library from thioglycollate-elicited macrophages of B10.A mice. On restriction mapping and sequencing analysis, we found three different genes and one cDNA clone coding for p91A-related molecules (Figs. 2 and 3A). One of the isolated genes was found to contain exons coding for the cytoplasmic portion harboring ITIM or ITIM-like sequences, suggesting that this is the gene for p91A. Interestingly, the amino acid sequence deduced from the second genomic DNA and a cDNA showed similar six Ig-like extracellular domains, but it contained unique pre-transmembrane, transmembrane and short cytoplasmic sequences harboring no ITIM or ITIM-like core structures (Fig. 3A). In addition, their transmembrane domains contain a positively charged residue, arginine, suggesting their association with other transmembrane proteins presumably critical for expression on the cell surface and for delivery of the activation signal, as is the case for FcγRIII and FcRγ interactions (*4–6*). The third genomic clone turned out to harbor only the 5′ part of a p91 gene (see Fig. 2), but its nucleotide sequence was quite similar, but definitely different from that of the second genomic clone. Thus, we assign these two p91 genes, different from p91A, as p91B and p91C.

Recently, Kubagawa *et al.* (*44*) reported the isolation of closely-related cDNA sequences coding for paired inhibitory receptors (PIR) from a BALB/c mouse library. These sequences show very high sequence homology to our p91 molecules (92–99% homology at the amino acid sequence level), suggesting that our p91 molecules and those of PIR are members of an identical family. Therefore, the present observations indicate that p91 (or PIR) comprises a multigene family, which includes a potent inhibitory p91A gene, and possibly noninhibitory or activatory p91B and p91C genes, although the accurate overall number of constituents of the noninhibitory-type molecules within the family remains to be clarified.

The p91 family is reminiscent of other groups of molecules such as human KIR and mouse gp49. For example, mouse gp49 has two isoforms. One is gp49A, that has no ITIM structure (*27*), whereas gp49B1 has two ITIM sequences (*28, 45*). gp49A has been speculated to play an

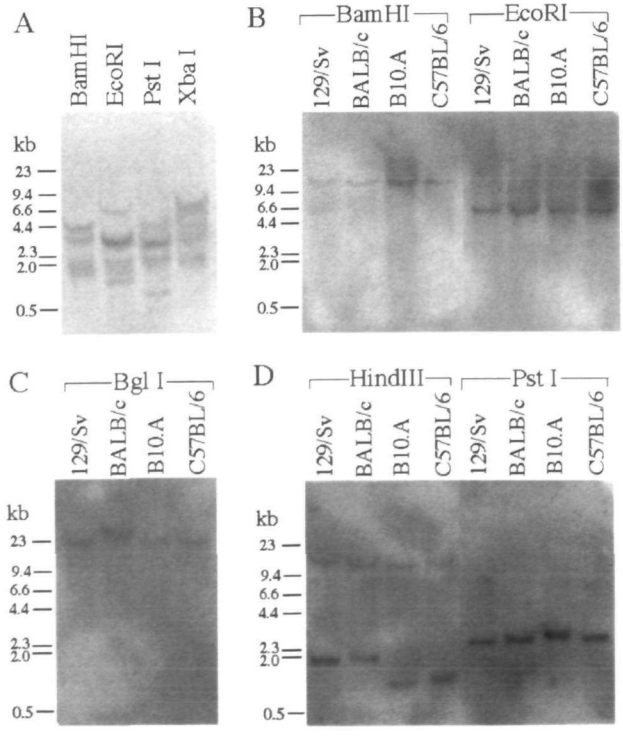

Fig. 1. **Southern blot analysis of the p91 gene family.** A mouse DNA sample digested with restriction enzyme was analyzed with p91 probes corresponding to the extracellular portion (panel A) and the cytoplasmic portion (panels B to D) of p91A. The DNA in panel A was from 129/Sv mice whereas that in panels B to D was derived from four different strains of mice, as indicated.

important role in cellular activation after co-expression with any signaling molecule (*45*). The deduced amino acid sequences of gp49A and gp49B1 proteins show multiple substitutions in their extracellular portions (*46*). The finding that the C57BL/6 allele of gp49B1 is identical to the C3H allele suggested minimal to no allelic polymorphism (*30*). In the present study, to our surprise, the extracellular portions of p91 molecules showed multiple substitutions of amino acid residues, especially in their first four extracellular domains (Fig. 3A), as was found for PIR (*44*). Moreover, it should be emphasized that allelic polymorphisms at 24 amino-acid positions in total have been observed in the deduced amino acid sequences of p91A (or PIR-B), a unique inhibitory-type p91 from three different strains of mice, *i.e.* 129/Sv, B10.A, and BALB/c. On the other hand, only one allelism was found in their cytoplasmic portions (Fig. 3A). It is unlikely that these three genes are not allelic because the p91A gene has been identified as a unique gene in the mouse genome (Fig. 1, B to D). Human KIR molecules have also been shown to contain many polymorphic substitutions in their extracellular domains (*18*).

Analysis of Cellular Components Associated with the Cytoplasmic Domain of p91A—p91A has four ITIM-like core sequences in its cytoplasmic domain (*25*). Their sequences are SLYASV (in the one-letter code), ETYAQV, VTYAQL, and SVYATL, from the N- to the C-terminus: they are separated by 23, 46, and 24 amino acid residues, respectively. The third sequence matches the ITIM consensus, V/I-X-Y-X-X-L/V (*11, 18, 45*), at stringent criteria. The question arises of whether these ITIM or ITIM-like sequences of p91A actually function as inhibitory motifs that interact with a cellular component or not. To address this issue, we attempted to detect cellular proteins associated with these sequences by immunoblot analysis. A whole cell lysate of mouse peritoneal macrophages or B lymphoma A20 cells was incubated with a tyrosine-phosphorylated or non-phosphorylated peptide matching each ITIM

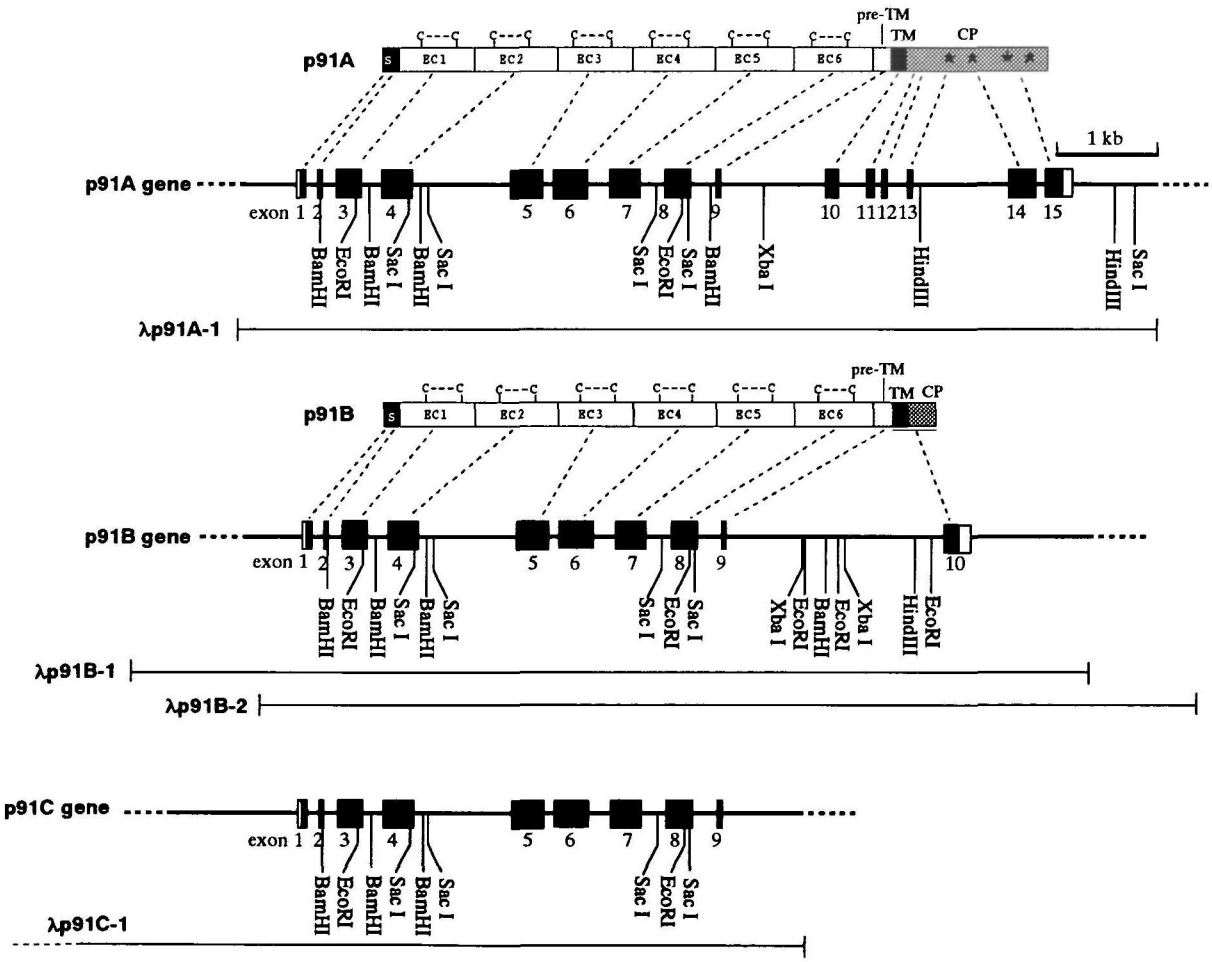

Fig. 2. **Schematic structures of genomic DNAs and diagram of the predicted protein domains.** Schematic representation of the exon/intron structures of p91A and p91B/C genes, and the corresponding protein domains are shown. The protein-coding sequences are denoted as closed boxes, and the non-coding sequences as open boxes. The relative positions of the isolated genomic clones are shown below each restriction map. Although the 3′ part of the p91C genomic clone has not yet been isolated due to it being almost identical in sequence to the p91B gene (see Fig. 3A), it should be emphasized that the restriction mapping and nucleotide sequence analyses of the isolated clone indicated that it is very closely related to, but not identical to the p91B gene. The protein structure is subdivided into the signal peptide (S), extracellular Ig-like domains (EC1 to EC6), and pretransmembrane (pre-TM), transmembrane (TM), and cytoplasmic (CP) domains. The positions of the 12 cysteines forming potential disulfide bonds (C-C) in the extracellular domain are shown. Stars indicate the positions of the ITIM-like core sequences.

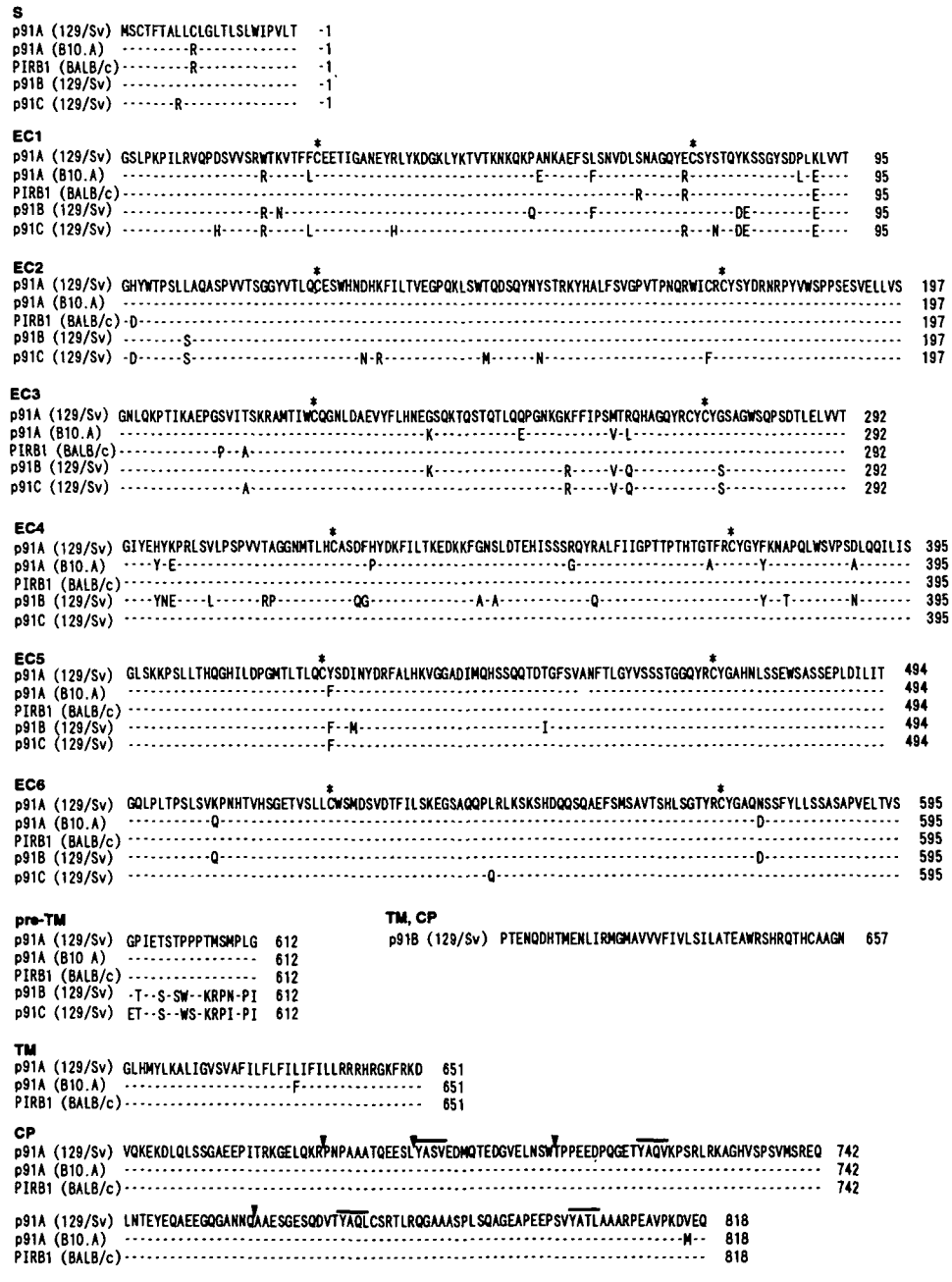

Fig. 3. **Alignment of the deduced amino acid sequences of p91 and PIR-B, and the human p91-like molecule (ILT4) and ILT1.** Alignment of the amino acid sequences of p91 proteins including PIR-B (panel A), and those of the human p91-like molecule and ILT1 (panel B) are shown, with subdivision into the signal peptide (S), extracellular Ig-like domains (EC1 to EC6), and pretransmembrane (pre-TM), transmembrane (TM), and cytoplasmic (CP) domains. Dashes indicate the identical residues. Asterisks denote the conserved cysteine residues involved in potential disulfide bonds. The position numbers of the residues are given on the right side of each line. Repeats of the ITIM-like core sequences, Y-X-X-L/V, are overlined. In CP of p91A, the positions of the introns are indicated by arrowheads.

or ITIM-like sequence found in the cytoplasmic portion of p91A, as described under "EXPERIMENTAL PROCEDURES." The bound proteins were analyzed with rabbit IgG to SHP-1 or SHP-2, and antiserum to SHIP. As shown in Fig. 4A, anti-SHP-1 and anti-SHP-2 antibodies detected ~65- and ~70-kDa proteins, respectively, associated with both phosphorylated pY3 and pY4, whereas anti-SHIP antibodies detected a ~145-kDa protein bound to phosphorylated pY3. Therefore, we concluded that both the third ITIM and the fourth ITIM-like sequences are able to bind SHP-1 and SHP-2, whereas the third ITIM sequence can also associate with SHIP from murine macrophages and B lymphoma cells upon phosphorylation of their tyrosine residues. It is interesting to note that the third ITIM shows significant sequence similarity to the second ITIM found in the gp49B1 cytoplasmic portion (*25*). Also, we found the association of SHP with the phosphorylated fourth ITIM-like sequence. Although the core sequence, SVYATL, does not satisfy the ITIM consensus sequence at stringent criteria, it is highly homologous to the cytoplasmic tyrosine-containing sequence, SIYSTL, of the mast cell function-associated antigen (MAFA). MAFA belongs to the C-type lectin family, expressed on rat RBL cells, and becomes phosphorylated and inhibits IgE-induced activation when aggregated (*47*). Thus, our finding suggests that this serine-containing motif also plays a critical role in the delivery of a negative signal, although the precise mechanism underlying the MAFA's inhibitory effect has not yet been elucidated.

Since these associations of SHP-1, SHP-2, and SHIP with the motifs are phosphorylation-dependent, we tried to verify that the p91A molecule could be phosphorylated at its cytoplasmic portion. Thioglycollate-elicited peritoneal macrophages were incubated in the presence of pervanadate, a tyrosine phosphatase inhibitor, and then were lysed, immunoprecipitated with anti-p91A antibodies (*25*), and analyzed by immunoblotting using anti-phosphotyrosine monoclonal antibodies. As shown in Fig. 4B, ~130-kDa p91A was not phosphorylated in intact cells but tyrosine-phosphorylated on inhibition of tyrosine phosphatases with pervanadate. Therefore, p91A could be a substrate for tyrosine phosphatases. It is suggested that tyrosine phosphorylation of the cytoplasmic domain of p91A, possibly within the ITIM sequences, is a prerequisite for the recruitment of SHP-1, SHP-2, and SHIP in macrophages, although the nature of the enzymes phosphorylating the tyrosine residues in the cytoplasmic domain of p91A remains to be clarified.

Detection of p91 mRNA in Mouse Tissues—On RNA blot analysis, we showed previously that p91A mRNA is expressed in macrophages and mast cells (*25*). To address the question of whether the mRNAs for inhibitory p91A and the noninhibitory or possibly activating p91B/C molecules are expressed differently or synchronously, we performed RT-PCR analysis of p91 mRNA expression in various

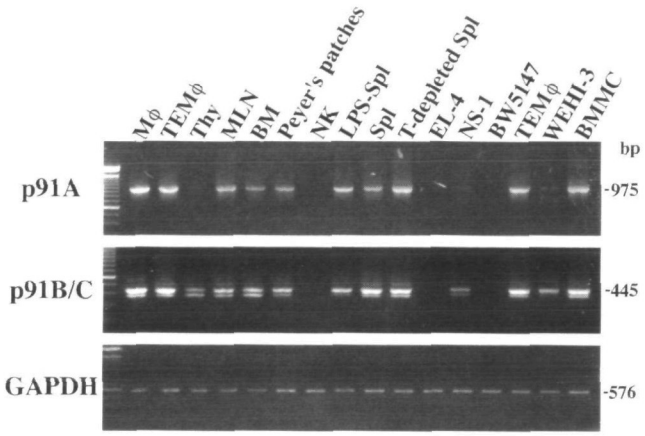

Fig. 5. **RT-PCR detection of p91 mRNA in various mouse tissues and cultured cells.** p91A and p91B/C cDNA fragments were selectively amplified by RT-PCR from total RNA obtained from each mouse tissue or cell line, and the amplified products were visualized by ethidium bromide staining. Bottom panel, GAPDH control. RNA samples were prepared from the following cells or tissues: (from left to right) peritoneal residential macrophages, thioglycollate-elicited peritoneal macrophages (TEMϕ), thymocytes, mesenteric lymph node cells, bone-marrow cells, Peyer's patch cells, splenic NK cells induced by IL-2 stimulation (all of these cells were isolated from C57BL/6 mice), lipopolysaccharide-stimulated splenocytes, splenocytes, and T-depleted splenocytes (from B10.A mice), T lymphoma EL-4 (C57BL/6), myeloma NS-1 (BALB/c), T lymphoma BW5147 (AKR/J), TEMϕ (B10.A), myelomonocyte WEHI-3 (BALB/c), and bone-marrow-derived cultured mast cells (B10.A).

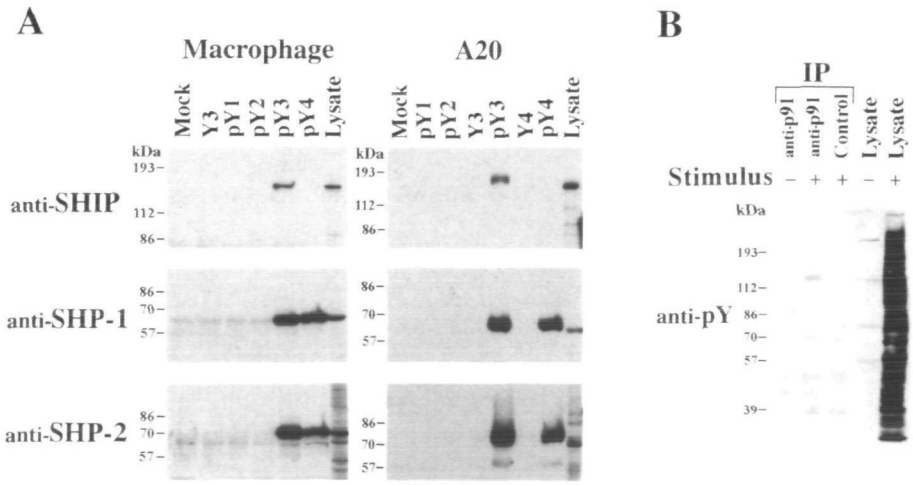

Fig. 4. **Immunoblot analysis of the proteins associated with phosphotyrosyl ITIM-like sequences of p91A.** Panel A, macrophage or A20 lysates were adsorbed with the indicated peptides. Affinity-bound proteins were resolved on 7.5% SDS-PAGE and probed with rabbit anti-SHIP antiserum, anti-SHP-1 IgG, or anti-SHP-2 IgG. Mock indicates mock affinity-isolation without any peptide but with avidin-Sepharose. Lysate indicates a total cell lysate without any adsorption. Panel B, macrophages were stimulated (+) or not stimulated (−) with 150 mM sodium pervanadate for 3 min. The cell lysates were prepared and resolved on 7.5% SDS-PAGE or immunoprecipitated using anti-p91 peptide 2 antiserum (*25*). The immunoblot was probed with anti-phosphotyrosine monoclonal antibodies. Lysate indicates a total cell lysate without immunoprecipitation.

mouse tissues and cells (Fig. 5). Sets of PCR primers were designed so as to discriminate between p91A and p91B/C cDNAs. As a result, we found that mRNAs for both the inhibitory isoform and the possibly activating isoforms were co-expressed in myeloid cells such as macrophages and mast cells, and also co-expressed in B cells, but not in T or NK cells. These expression patterns were quite similar to those of FcγRIIB (*2*) and immunoglobulin-like transcripts (ILT) (*31*). Recently, Meyaard *et al.* (*48*) described a novel inhibitory receptor, leukocyte-associated immunoglobulin-like receptor-1 (LAIR-1), that is constitutively expressed on the majority of human peripheral blood mononuclear leukocytes. Although the overall homology of LAIR-1 with p91 is less than 30%, LAIR-1 shows slightly higher homology (32%) to ILT (*48*), suggesting the presence of a novel family of highly related receptors, similar to the situations of ILT, KIR, gp49, and p91.

Chromosomal Mapping of Mouse p91—The chromosomal assignment of the p91 genes was performed by direct R-banding FISH using mouse genomic and cDNA fragments for mouse chromosomes and a mouse cDNA fragment for rat chromosomes as probes. The p91 genes were localized to the proximal end of mouse chromosome 7, which is a syntenic position of human chromosome 19

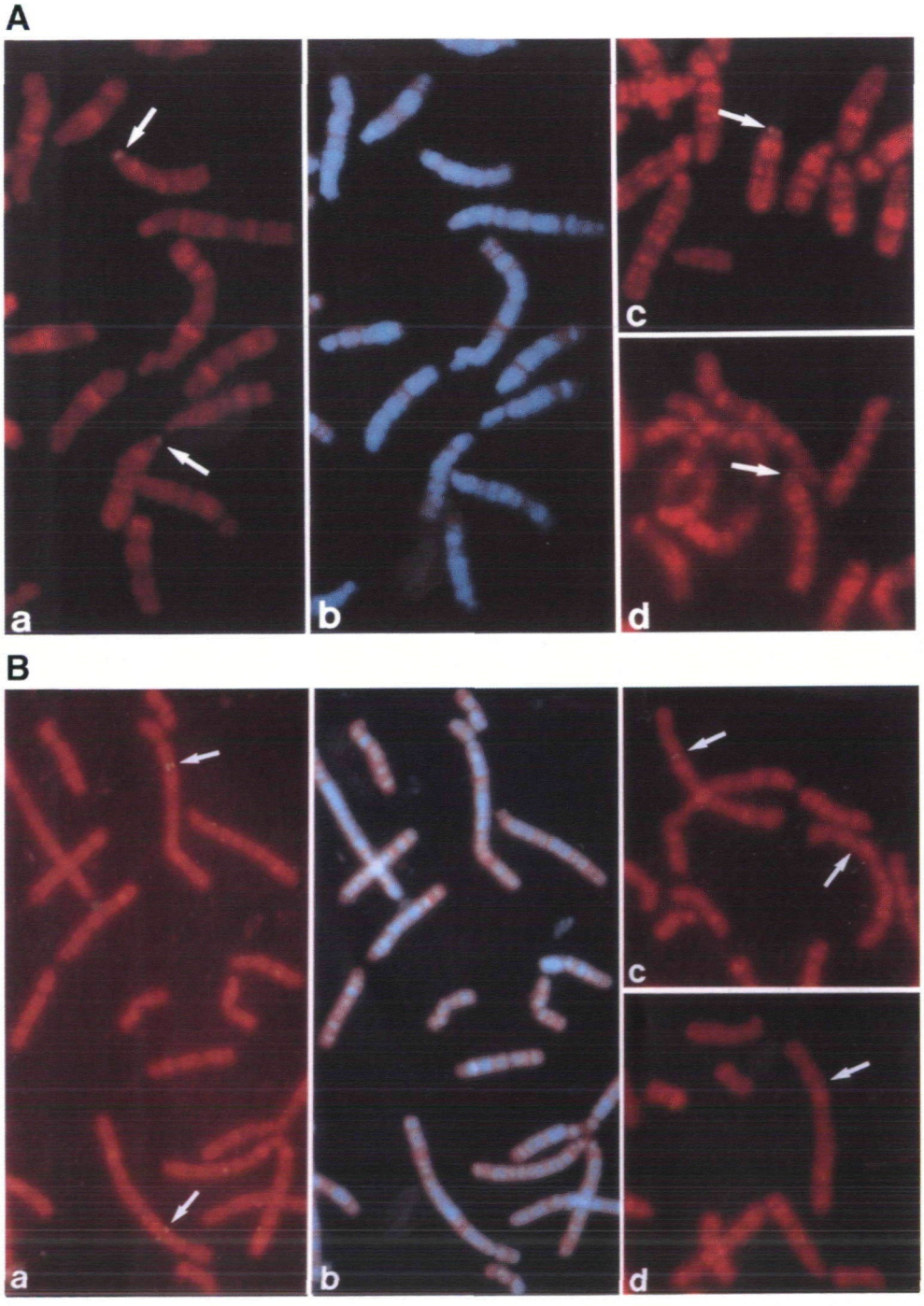

Fig. 6. **Chromosomal localization of the p91 genes on R-banded mouse (A) and rat (B) chromosomes.** Panel A, the chromosomal location of the mouse p91 genes was determined by using 16-kb p91C genomic (a, b, c) and 0.9-kb p91A cDNA (d) fragments as biotinylated probes. The hybridization signals are indicated by arrows. The signals are localized to the proximal end of mouse chromosome 7. The metaphase spreads were photographed with Nikon B-2A (a, c, d) and UV-2A (b) filters. R-band and G-band patterns are shown in (a, c, d) and (b), respectively. Panel B, the chromosomal location of the rat p91 genes was determined by using a 0.9-kb mouse p91A cDNA fragment as a biotinylated probe. The hybridization signals are indicated by arrows. The signals are localized to the distal end of q21.1—the proximal end of q21.3 on rat chromosome 1. The metaphase spreads were photographed with Nikon B-2A (a, c, d) and UV-2A (b) filters. R-band and G-band patterns are shown in (a, c, d) and (b), respectively.

where p58 KIR genes have been mapped (*18*), and the distal end of q21.1—the proximal end of q21.3 on rat chromosome 1, where conserved linkage homology to mouse chromosome 7 has been identified (*39, 49-52*) (Fig. 6).

Fine linkage mapping of the mouse p91 genes was performed by interspecific backcross analysis using progeny derived through the mating of (C57BL/6 × *M. spretus*) F_1 × *M. spretus* mice. The genomic DNAs of C57BL/6 and *M. spretus* were separately digested with six different restriction endonucleases, *Apa*I, *Bam*HI, *Eco*RI, *Hin*dIII, *Kpn*I, and *Pst*I, and then analyzed by Southern blot hybridization for informative RFLVs (restriction fragment length variants) using a 0.4-kb p91A cDNA fragment as a probe. RFLVs obtained on Southern blot hybridization between C57BL/6 and *M. spretus* were detected on digestion with *Apa*I, *Bam*HI, *Eco*RI, *Hin*dIII, *Kpn*I, and *Pst*I.

The RFLVs on *Pst*I-digestion, 8.2- and 5.8-kb fragments in C57BL/6, there being no fragments of these sizes in *M. spretus*, were used to follow the segregation of the p91

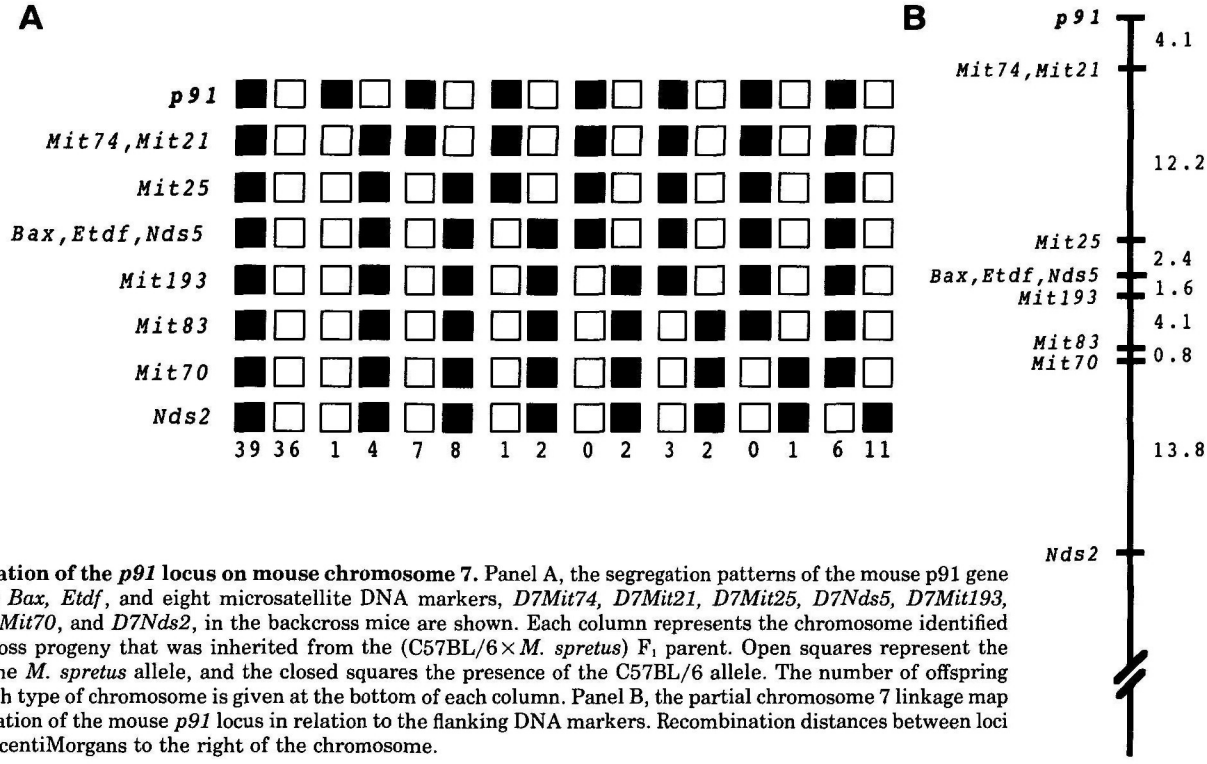

Fig. 7. **Location of the *p91* locus on mouse chromosome 7.** Panel A, the segregation patterns of the mouse p91 gene with flanking *Bax, Etdf*, and eight microsatellite DNA markers, *D7Mit74, D7Mit21, D7Mit25, D7Nds5, D7Mit193, D7Mit83, D7Mit70*, and *D7Nds2*, in the backcross mice are shown. Each column represents the chromosome identified in the backcross progeny that was inherited from the (C57BL/6 × *M. spretus*) F_1 parent. Open squares represent the presence of the *M. spretus* allele, and the closed squares the presence of the C57BL/6 allele. The number of offspring inheriting each type of chromosome is given at the bottom of each column. Panel B, the partial chromosome 7 linkage map shows the location of the mouse *p91* locus in relation to the flanking DNA markers. Recombination distances between loci are shown in centiMorgans to the right of the chromosome.

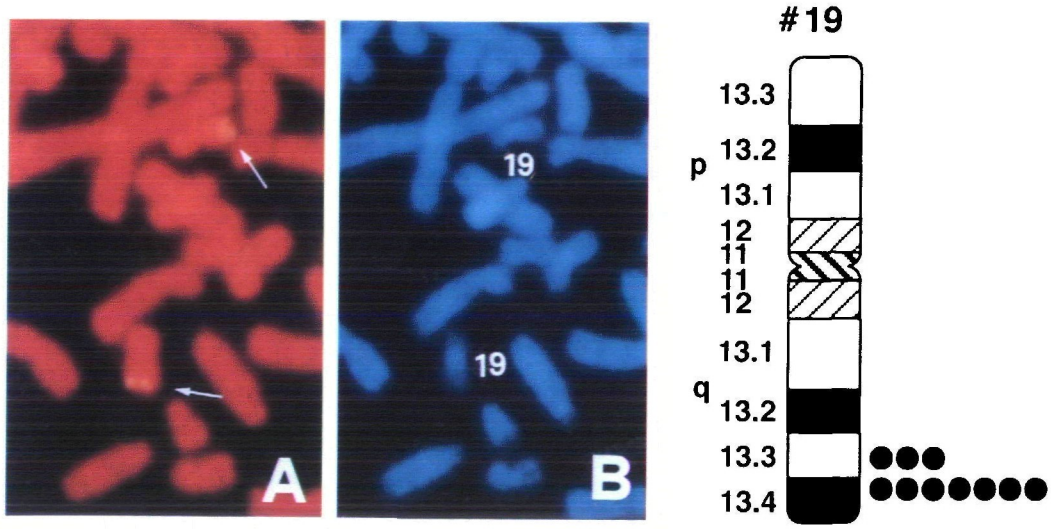

Fig. 8. **Chromosomal assignment of the gene for the human p91-like molecule (or ILT4).** Panel A, the FISH signals on chromosomes. Panel B, the same mitotic figure as in panel A, stained with DAPI to identify chromosome 19. In the schematic diagram of human chromosome 19, each dot represents a double FISH signal detected.

genotypes in a total of 123 interspecific backcross mice. We examined the concordance of the segregation of RFLVs identified on Southern blot hybridization with the segregation of *Bax* (*53*), *Etdf* (*54*), and eight microsatellite DNA markers, *D7Mit74, D7Mit21, D7Mit25, D7Nds5, D7Mit193, D7Mit83, D7Mit70*, and *D7Nds2*. The gene order was determined by minimizing the number of recombination events required to explain the allele distribution patterns. Comparative pairwise loci analysis showed that the gene order and recombination frequency, expressed as genetic distances in centiMorgan±standard error, and the number of recombinants, on chromosome 7 are: centromere-p91—4.1±1.8 (5/123)—*D7Mit74, D7Mit21* —12.2±3.0 (15/123)—*D7Mit25*—2.4±1.4 (3/123) —*Bax, Etdf, D7Nds5*—1.6±1.1 (2/123)—*D7Mit193* —4.1±1.8 (5/123)—*D7Mit83*—0.8±0.8 (1/123) —*D7Mit70*—13.8±3.1 (17/123)—*D7Nds2*-telomere (Fig. 7).

The present data suggest that the p91 locus is closer to the centromere than any other proximal loci reported in the previous papers (*50, 55*). We have compared our interspecific linkage map of mouse chromosomes 7 with a recent composite mouse linkage map, in which uncloned mouse mutations were localized (*50, 55*). Three mutations were identified around the position of the *p91* locus, *i.e.*, juvenile bare (*jb*, Ref. *56*), Nijmegen waltzer (*nv*, Ref. *57*), and reduced pigmentation (*rp*, Ref. *58*), but their relationships to p91 are unclear.

Isolation of a cDNA Clone for the Human p91-Like Molecule and Its Chromosomal Mapping—The finding of a novel group of mouse molecules, the p91 family, raises the question of whether or not p91 molecules are present in man. Therefore, we attempted to isolate human homologs of p91 by screening a human splenocyte cDNA library with mouse p91 as a probe. We characterized 4 positive clones (#1 to #4) for the hybridization using a probe corresponding to a common extracellular portion of p91, and found that one of them (#1) is a full-length cDNA clone with a 2.3-kb insert. Unexpectedly, a homology search revealed that this sequence was quite similar (amino-acid sequence identity of 92%, Fig. 3B) to that of human ILT1 isolated from a human NK cell line very recently (*31*). Although the three other cDNA clones characterized were not full-length, we observed that two of them (#2 and #3) were also nearly identical to human ILT1, the fourth clone (#4) was almost identical to ILT2 (nucleotide sequence homology of 95%). The extracellular portion of the human p91-like molecule (designated as ILT4) contained four Ig-like domains, a transmembrane region, and a short cytoplasmic sequence (Fig. 3B). ILT2 and ILT3 characterized by Samaridis and Colonna (*31*), and Cella *et al.* (*32*) contained a cytoplasmic domain harboring four and three ITIM or ITIM-like sequences, respectively. We verified that clone #4 possessed a sequence coding for these ITIM sequences of ILT2 (data not shown).

The chromosomal assignment of the gene for the human p91-like molecule (or ILT4) was performed by direct FISH using the human cDNA fragment as a probe. The hybridization efficiency was approximately 78% for this probe (among 100 mitotic figures checked 78 showed signals for one pair of the chromosomes). Since DAPI banding was used to identify the specific chromosome, the correspondence between the FISH signals and the long arm of chromosome 19 was obtained. The detailed position was further determined based on a summary of 10 photos (Fig. 8). There was no additional locus revealed on FISH detection under the conditions used, therefore, the gene was found to be located on human chromosome 19, region q13.3-13.4. Region 19q13.4 is the position where the KIR genes have also been localized (*18, 59*). Thus, the gene for the human p91-like molecule (or ILT4) is very close to the position of KIR genes. It would be interesting to determine how far apart the human KIR and ILT families are from the viewpoint of gene evolution. Based on the striking similarity in their structures (Fig. 3B) and the expression pattern (Fig. 5, Ref. *31*), and on the chromosomal mapping data described above (Fig. 8), we propose that the ILTs are human p91-like molecules, although the numbers of extracellular Ig-domains are different in these molecules from the two species.

The results of our analyses of the structural characteristics of p91 molecules and the potent inhibitory nature of p91A strongly suggested that products derived from the gene family should be important as a set of regulatory receptors expressed on myeloid cells and B cells. Although the ligand for p91 is not known, and detailed information on their inhibitory and activating signaling cascades is still lacking, elucidation of the molecular mechanisms underlying p91 functions should be valuable for understanding how cell responsibilities as to external stimuli are controlled by surface receptors.

REFERENCES

1. Ravetch, J.V. (1994) Fc receptors: Rubor redux. *Cell* **78**, 553-560
2. Ravetch, J.V. and Kinet, J.-P. (1991) Fc receptors. *Annu. Rev. Immunol.* **9**, 457-492
3. Reth, M. (1989) Antigen receptor tail clue. *Nature* **338**, 383
4. Kurosaki, T. and Ravetch, J.V. (1989) A single amino acid in the glycosyl phosphatidylinositol attachment domain determines the membrane topology of FcγRIII. *Nature* **342**, 805-807
5. Kurosaki, T., Gander, I., and Ravetch, J.V. (1991) A subunit common to an IgG Fc receptor and the T-cell receptor mediates assembly through different interactions. *Proc. Natl. Acad. Sci. USA* **88**, 3837-3841
6. Wirthmueller, U., Kurosaki, T., Murakami, M., and Ravetch, J.V. (1992) Signal transduction by FcγRIII (CD16) is mediated through the γ-chain. *J. Exp. Med.* **175**, 1381-1390
7. Daeron, M., Latour, S., Malbec, O., Espinosa, E., Pina, P., Pasmans, S., and Fridman, W.H. (1995) The same tyrosine-based inhibition motif, in the intracytoplasmic domain of FcγRIIB, regulates negatively BCR-, TCR-, and FcR-dependent cell activation. *Immunity* **3**, 635-646
8. Thomas, M.L. (1995) Of ITAMs and ITIMs: turning on and off the B cell antigen receptor. *J. Exp. Med.* **181**, 1953-1956
9. Amigorena, S., Bonnerot, C., Drake, J.R., Choquet, D., Hunziker, W., Guillet, J.G., Webster, P., Sautes, C., Mellman, I., and Fridman, W.H. (1992) Cytoplasmic domain heterogeneity and functions of IgG Fc receptors in B lymphocytes. *Science* **256**, 1808-1812
10. Muta, T., Kurosaki, T., Misulovin, Z., Sanchez, M., Nussenzweig, M.C., and Ravetch, J.V. (1994) A 13-amino-acid motif in the cytoplasmic domain of FcγRIIB modulates B-cell receptor signalling. *Nature* **368**, 70-73
11. Burshtyn, D.N., Scharenberg, A.M., Wagtman, N., Rajagopalan, S., Berrada, K., Yi, T., Kinet, J.-P., and Long, E.O. (1996) Recruitment of tyrosine phosphatase HCP by the killer cell inhibitor receptor. *Immunity* **4**, 77-85
12. D'Ambrosio, D., Hippen, K.L., Minskoff, S.A., Mellman, I., Pani, G., Siminovitch, K.A., and Cambier, J.C. (1995) Recruitment and activation of PTP1C in negative regulation of antigen receptor signaling by FcγRIIB1. *Science* **268**, 293-297
13. Ono, M., Bolland, S., Tempst, P., and Ravetch, J.V. (1996) Role of the inositol phosphatase SHIP in negative regulation of the immune system by the receptor FcγRIIB. *Nature* **383**, 263-266

14. Leibson, P.J. (1997) Signal transduction during natural killer cell activation: inside the mind of a killer. *Immunity* **6**, 655-661
15. Long, E.O. and Burshtyn, D.N. (1997) Killer cell inhibitory receptors: diversity, specificity, and function. *Immunol. Rev.* **155**, 135-144
16. Lanier, L.L. and Phillips, J.H. (1996) Inhibitory MHC class I receptor on NK cells and T cells. *Immunol. Today* **17**, 86-91
17. Raulet, D.H. and Held, W. (1995) Natural killer cell receptors: the offs and ons of NK cell recognition. *Cell* **82**, 697-700
18. Wagtmann, N., Biassoni, R., Cantoni, C., Verdiani, S., Malnati, M.S., Vitale, M., Bottino, C., Moretta, L., Moretta, A., and Long, E.O. (1995) Molecular clones of the p58 NK cell receptor reveal immunoglobulin-related molecules with diversity in both the extra- and intracellular domains. *Immunity* **2**, 439-449
19. Colonna, M. and Samaridis, J. (1995) Cloning of immunoglobulin-superfamily members associated with HLA-C and HLA-B recognition by human natural killer cells. *Science* **268**, 405-408
20. D'Andrea, A., Chang, C., Franz-Bacon, K., McClanahan, T., Phillips, J., and Lanier, L.L. (1995) Molecular cloning of NKB1. A natural killer cell receptor for HLA-B allotypes. *J. Immunol.* **155**, 2306-2310
21. Chang, C., Rodriguez, A., Carretero, M., Lopez-Botet, M., Phillips, J.H., and Lanier, L.L. (1995) Molecular characterization of human CD94: a type II membrane glycoprotein related to the C-type lectin superfamily. *Eur. J. Immunol.* **25**, 2433-2437
22. Yokoyama, W.M. and Seaman, W.E. (1993) The Ly-49 and NKR-P1 gene families encoding lectin-like receptors on natural killer cells: the NK gene complex. *Annu. Rev. Immunol.* **11**, 613-635
23. Campbell, K.S., Dessing, M., Lopez-Botet, M., Cella, M., and Colonna, M. (1996) Tyrosine phosphorylation of a human killer inhibitory receptor recruits protein tyrosine phosphatase 1C. *J. Exp. Med.* **184**, 93-100
24. Olcese, L., Lang, P., Vely, F., Cambiaggi, A., Marguet, D., Blery, M., Hippen, K.L., Biassoni, R., Moretta, A., Moretta, L., Cambier, J.C., and Vivier, E. (1996) Human and mouse killer-cell inhibitory receptors recruit PTP1C and PTP1D protein tyrosine phosphatases. *J. Immunol.* **156**, 4531-4534
25. Hayami, K., Fukuta, D., Nishikawa, Y., Yamashita, Y., Inui, M., Ohyama, Y., Hikida, M., Ohmori, H., and Takai, T. (1997) Molecular cloning of a novel murine cell-surface glycoprotein homologous to killer cell inhibitory receptors. *J. Biol. Chem.* **272**, 7320-7327
26. Katz, H.R., Benson, A.C., and Austen, K.F. (1989) Activation- and phorbol ester-stimulated phosphorylation of a plasma membrane glycoprotein antigen expressed on mouse IL-3-dependent mast cells and serosal mast cells. *J. Immunol.* **142**, 919-926
27. Arm, J.P., Gurish, M.F., Reynolds, D.S., Scott, H.C., Gartner, C.S., Austen, K.F., and Katz, H.R. (1991) Molecular cloning of gp49, a cell-surface antigen that is preferentially expressed by mouse mast cell progenitors and is a new member of the immunoglobulin superfamily. *J. Biol. Chem.* **266**, 15966-15973
28. Katz, H.R., Vivier, E., Castells, M.C., McCormick, M.J., Chambers, J.M., and Austen, K.F. (1996) Mouse mast cell gp49B1 contains two immunoreceptor tyrosine-based inhibition motifs and suppresses mast cell activation when coligated with the high-affinity Fc receptor for IgE. *Proc. Natl. Acad. Sci. USA* **93**, 10809-10814
29. Rojo, S., Burshtyn, D.N., Long, E.O., and Wagtmann, N. (1997) Type I transmembrane receptor with inhibitory function in mouse mast cells and NK cells. *J. Immunol.* **158**, 9-12
30. Wang, L.L., Mehta, I.K., LeBlanc, P.A., and Yokoyama, W.M. (1997) Mouse natural killer cells express gp49B1, a structural homologue of human killer inhibitory receptors. *J. Immunol.* **158**, 13-17
31. Samaridis, J. and Colonna, M. (1997) Cloning of novel immunoglobulin superfamily receptors expressed on human myeloid and lymphoid cells: structural evidence for new stimulatory and inhibitory pathways. *Eur. J. Immunol.* **27**, 660-665
32. Cella, M., Dohring, C., Samaridis, J., Dessing, M., Brockhous, M., Lanzavecchia, A., and Colonna, M. (1997) A novel inhibitory receptor (ILT-3) expressed on monocytes, macrophages, and dendritic cells involved in antigen processing. *J. Exp. Med.* **185**, 1743-1751
33. Sambrook, J., Fritsch, E.F., and Maniatis, T. (1989) *Molecular Cloning: A Laboratory Manual*, 2nd ed., Cold Spring Harbor Laboratory, Cold Spring Harbor, NY
34. Takai, T., Li, M., Sylvestre, D., Clynes, R., and Ravetch, J.V. (1994) FcR γ chain deletion results in pleiotrophic effector cell defects. *Cell* **76**, 519-529
35. Sanger, F., Nicklen, S., and Coulson, A.R. (1977) DNA sequencing with chain-terminating inhibitors. *Proc. Natl. Acad. Sci. USA* **74**, 5463-5467
36. Chomczynski, P. and Sacchi, N. (1987) Single-step method of RNA isolation by acid guanidinium thiocyanate-phenol-chloroform extraction. *Anal. Biochem.* **162**, 156-159
37. Kim, K., Kanellopoulos-Langevin, C., Merwin, R., Sachs, D., and Asofsky, R.(1979) Establishment and characterization of BALB/c lymphoma lines with B cell properties. *J. Immunol.* **122**, 549-554
38. Singh, S., Darnay, B.G., and Aggarwal, B.B. (1996) Site-specific tyrosine phosphorylation of IκBα negatively regulates its inducible phosphorylation and degradation. *J. Biol. Chem.* **271**, 31049-31054
39. Matsuda, Y., Harada, Y.-N., Natsuume-Sakai, S., Lee, K., Shiomi, T., and Chapman, V.M. (1992) Location of the mouse complement factor H gene (*cfh*) by FISH analysis and replication R-banding. *Cytogenet. Cell Genet.* **61**, 282-285
40. Matsuda, Y. and Chapman, V.M. (1995) Application of fluorescence *in situ* hybridization in genome analysis of the mouse. *Electrophoresis* **16**, 261-272
41. Heng, H.H.Q., Squire, J., and Tsui, L.-C. (1992) High resolution mapping of mammalian genes by *in situ* hybridization to free chromatin. *Proc. Natl. Acad. Sci. USA* **89**, 9509-9513
42. Heng, H.H.Q. and Tsui, L.-C. (1993) Modes of DAPI banding and simultaneous *in situ* hybridization. *Chromosoma* **102**, 325-332
43. Matsuda, Y., Imai, T., Shiomi, T., Saito, T., Yamauchi, M., Fukao, T., Akao, Y., Seki, N., Ito, T., and Hori, T. (1996) Comparative genome mapping of the ataxia-telangiectasia region in mouse, rat and Syrian hamster. *Genomics* **34**, 347-357
44. Kubagawa, H., Burrows, P.D., and Cooper, M.D. (1997) A novel pair of immunoglobulin-like receptors expressed by B cells and myeloid cells. *Proc. Natl. Acad. Sci. USA* **94**, 5261-5266
45. Katz, H.R. and Austen, K.F. (1997) A newly recognized pathway for the negative regulation of mast cell-dependent hypersensitivity and inflammation mediated by an endogenous cell surface receptor of the gp49 family. *J. Immunol.* **158**, 5065-5070
46. Castells, M.C., Wu, X., Arm, J.P., Austen K.F., and Katz, H.R. (1994) Cloning of the gp49B gene of the immunoglobulin superfamily and demonstration that one of its two products is an early-expressed mast cell surface protein originally described as gp49. *J. Biol. Chem.* **269**, 8393-8401
47. Guthmann, M.D., Tal, M., and Pecht, I. (1995) A secretion inhibitory signal transduction molecule on mast cells is another C-type lectin. *Proc. Natl. Acad. Sci. USA* **92**, 9397-9401
48. Meyaard, L., Adema, G.J., Chang, C., Woollatt, E., Sutherland, G.R., Lanier, L.L., and Phillips, J.H. (1997) LAIR-1, a novel inhibitory receptor expressed on human mononuclear leukocytes. *Immunity* **7**, 283-290
49. Lyon, M.F., Cocking, Y., and Gao, X. (1997) Mouse chromosome atlas. *Mouse Genome* **95**, 29-78
50. Satoh, H., Yoshida, M.C., and Sasaki, M. (1989) High resolution chromosome banding in the Norway rat, *Rattus norvegicus*. *Cytogenet. Cell Genet.* **50**, 151-154
51. Somssich, I.E. and Hameister, H. (1996) Standard karyotype of early replicating bands (RBG-banding) in *Genetic Variants and Strains of the Laboratory Mouse* (Lyon, M.F., Rastan, S., and Brown, S.D.M., eds.) pp. 1450-1451, Oxford University Press, Oxford
52. Yamada, J., Kuramoto, T., and Serikawa, T. (1994) A rat genetic linkage map and comparative maps for mouse or human homologous rat genes. *Mammal. Genome* **5**, 63-83
53. Matsuda, Y., Kusano, H., and Tsujimoto, Y. (1996) Chromosomal assignment of the Bcl2-related genes, Bcl21 and Bax, in the mouse and rat. *Cytogenet. Cell Genet.* **74**, 107-110
54. Suzuki, K., Yasunami, M., Matsuda, Y., Maeda, T., Kobayashi, H., Terasaki, H., and Ohkubo, H. (1996) Structural organization and chromosomal assignment of mouse embryonic TEA domain-containing factor (ETF) gene. *Genomics* **36**, 263-270
55. Brilliant, M.H., Williams, R.W., Holdener, B.C., and Angel, J. M. (1996) Mouse chromosome 7. *Mammal. Genome* (*Special Issue*) **6**, S135-S150
56. Lane, P.W., Taylor, B.A., Davisson, M.T., Cook, S., and Rowe, L. (1989) Juvenile bare (*jb*). *Mouse News Lett.* **83**, 166
57. van Abeelen, J.H.F. and Kalkhoven, J.Th.R. (1970) Behavioural ontogeny of the Nijmegen waltzer, a neurological mutant in the mouse. *Anim. Behav.* **18**, 711-718
58. Orn, A., Hakansson, E.M., Gidlund, M., Ramstedt, U., Axberg, I., Wigzell, H., and Lundin, L.-G. (1982) Pigment mutations in the mouse which also affect lysosomal functions lead to suppressed natural killer cell activity. *Scand. J. Immunol.* **15**, 305-310
59. Baker, E., D'Andrea, A., Phillips, J.H., Sutherland, G.R., and Lanier, L.L. (1995) Natural killer cell receptor for HLA-B allotypes, NKB1: Map position 19q13.4. *Chromosome Res.* **3**, 511